

Article

Improved Hydrogen Peroxide Stress Resistance of *Zymomonas mobilis* NADH Dehydrogenase (*ndh*) and Alcohol Dehydrogenase (*adhB*) Mutants

Kristiana Kovtuna, Inese Strazdina, Mara Bikerniece, Nina Galinina, Reinis Rutkis, Jekaterina Martynova and Uldis Kalnenieks *

Institute of Microbiology and Biotechnology, University of Latvia, LV-1586 Riga, Latvia; kristiana.kovtuna@lu.lv (K.K.); inese.strazdina@lu.lv (I.S.); mara.bikerniece@gmail.com (M.B.); nina.galinina@lu.lv (N.G.); reinis.rutkis@lu.lv (R.R.); jek.martynova@gmail.com (J.M.)

* Correspondence: uldis.kalnenieks@lu.lv



Citation: Kovtuna, K.; Strazdina, I.; Bikerniece, M.; Galinina, N.; Rutkis, R.; Martynova, J.; Kalnenieks, U. Improved Hydrogen Peroxide Stress Resistance of *Zymomonas mobilis* NADH Dehydrogenase (*ndh*) and Alcohol Dehydrogenase (*adhB*) Mutants. *Fermentation* **2022**, *8*, 289. <https://doi.org/10.3390/fermentation8060289>

Academic Editors: Alexander Rapoport, John E. Hallsworth, Justyna Ruchala and Tiffany D. Dallas

Received: 25 May 2022

Accepted: 17 June 2022

Published: 19 June 2022

Publisher's Note: MDPI stays neutral with regard to jurisdictional claims in published maps and institutional affiliations.



Copyright: © 2022 by the authors. Licensee MDPI, Basel, Switzerland. This article is an open access article distributed under the terms and conditions of the Creative Commons Attribution (CC BY) license (<https://creativecommons.org/licenses/by/4.0/>).

Abstract: Unintended shifts in stress resistance of microbial strains with engineered central metabolism may impact their growth and production performance under oxidative, lignocellulosic, solvent, and other stress conditions, and as such, must be taken into account in bioprocess design. In the present work, we studied oxidative stress resistance in mutant strains of the facultatively anaerobic, ethanologenic bacterium *Zymomonas mobilis* with modified respiratory (inactivated NADH dehydrogenase Ndh, by disruption of *ndh*) and ethanologenic (inactivated iron-containing alcohol dehydrogenase isoenzyme ADH II, by disruption of *adhB*) catabolism, using exogenously added H₂O₂ in the concentration range of 2–6 mM as the oxidative stressor. Both mutations improved H₂O₂ resistance and enhanced catalase activity by a factor of 2–5, while the overexpression of Ndh had an opposite effect. Strains with a catalase-negative background were unable to grow already at 1 mM hydrogen peroxide, and their H₂O₂ resistance did not depend on AdhB or Ndh expression levels. Hence, the improved resistance of the *ndh* and *adhB* mutants to H₂O₂ resulted from their elevated catalase activity. The interrelation between these mutations, the catabolic redox balance, catalase activity, and oxidative stress defense in *Z. mobilis* is discussed.

Keywords: *Zymomonas mobilis*; hydrogen peroxide resistance; alcohol dehydrogenase; respiratory NADH dehydrogenase; oxidative stress

1. Introduction

Zymomonas mobilis is a facultatively anaerobic alpha-proteobacterium, known for its powerful ethanol fermentation pathway, which involves the Entner–Doudoroff (E–D) glycolysis in combination with pyruvate decarboxylase (Pdc) and two alcohol dehydrogenase (ADH) isoenzymes—zinc-containing ADH I (AdhA) and iron-containing ADH II (AdhB) [1,2]. This bacterium also possesses a constitutive aerobic respiratory chain, operating with a low energy-coupling efficiency, not contributing to oxidative ATP synthesis and biomass yield [3–6], yet bearing potential for the rapid regeneration of intracellular NAD(P)⁺ pools [7]. *Z. mobilis* is able to grow on glucose, fructose, sucrose, and complex sucrose-containing substrates, e.g., plant saps or molasses from the sugar industry [8,9], and synthesize ethanol as its major fermentation product with high specific rate and yield [1,2]. Besides, it can tolerate high sugar (up to 40%) and ethanol (up to 16%) concentrations [2,8] in the growth medium. These valuable properties have stimulated efforts in the *Z. mobilis* metabolic engineering of bioethanol production from various renewable substrates, primarily from lignocellulose hydrolysates [10,11]. Apart from its natural capacity for ethanol production, the catabolism of *Z. mobilis* has been recently engineered for the synthesis of alternative products, such as 2,3-butanediol [12], isobutanol [13], acetaldehyde [14], the TCA intermediates, and more (for reviews, see [15–17]).

The engineering of novel product pathways in *Zymomonas* is based on the redesign of its central metabolism; primarily the reactions around its pyruvate node, ADHs, and also, the respiratory chain. Although in many cases the desired result could thus be achieved, it is also becoming increasingly clear that manipulation of the microbial central metabolism may bring about unintended side effects. In particular, that concerns complex physiological properties, such as resistance to various types of stress. Since such effects are relevant for the metabolic engineering of producer strains, especially those that are confronted with industrial stress condition (such as thermal or oxidative stress), they need to be investigated and taken into account in novel bioprocess developments.

With *Z. mobilis*, telling examples of metabolic engineering side effects on stress resistance are the improved aerobic growth and the unexpected change of temperature and salt resistance properties in its *ndh* mutant strains [18–21]. In a number of bacteria, the energy non-coupling, type II NADH dehydrogenase (*ndh*) functions to maintain a low NADH/NAD ratio (for reviews, see, e.g., [22,23]), and its activity thus affects the product spectrum (aerobic accumulation of acetaldehyde), as well as the function of the redox-dependent ROS-protective systems. The activity of Ndh might also directly impact the electron supply to respiratory peroxidases. In *Z. mobilis*, a respiratory cytochrome *c*-dependent peroxidase PerC has been identified [24,25], and the sensitivity of its knock-out mutant Zm6-*perC* to H₂O₂ has been reported.

Moreover, the putative function of AdhB as a stress protein [26] implies unintended effects in *Z. mobilis adhB* mutants, which so far are poorly studied. The relation of the iron-containing alcohol dehydrogenases (ADHs) to microbial oxidative stress protection is well documented. The iron-dependent bifunctional aldehyde-alcohol dehydrogenases in a variety of bacteria, including *Escherichia coli* [27,28], *Acinetobacter baumannii* [29], *Streptococcus pneumoniae* [30], and *Bacillus cereus* [31], have been shown to contribute to oxidative stress resistance, and to virulence and biofilm forming ability as well. In some bacteria, iron dependent ADHs are represented by multiple isoenzymes [29], part of which might be functioning primarily in oxidative stress protection, but not in ethanol metabolism. The mutants deficient in these ADHs show impaired aerobic growth and elevated sensitivity to hydrogen peroxide. Perhaps, the best studied example here is the AdhE of *E. coli*, for which the protective role against submillimolar H₂O₂ concentrations has first been demonstrated by Echave et al. [27]. AdhE protects cells by scavenging H₂O₂ that leads to carbonylation and inactivation of the enzyme itself. Notably, the replacement of iron by zinc in the enzyme active center not only inactivates its alcohol dehydrogenase function, but also eliminates its H₂O₂ -scavenging ability. As a result, the cells become hypersensitive to hydrogen peroxide. Reactivity with H₂O₂ and comparable effects of iron replacement by zinc have been reported also for the AdhB of *Z. mobilis* [32]. Given that AdhB is induced in *Z. mobilis* by exposure to temperature or ethanol stress [26], it is tempting to suppose that it also should have a protective role against oxidative stress, akin to the ADHs discussed above.

In the present work we have examined oxidative stress resistance of *Z. mobilis* strains with disrupted *ndh* and/or *adhB*, using exogenously added H₂O₂ as the oxidative stressor. We show that these genetic modifications, which both decrease the catabolic NADH consumption rate and tend to elevate catalase expression, as a consequence, substantially improve the strain resistance to H₂O₂ in the millimolar concentration range.

2. Materials and Methods

2.1. Strains and Cultivation

Zymomonas mobilis strains used in the present study are listed in Table 1. The double knock-out mutant Zm6-*adhB-ndh* was constructed by transforming the cells of the strain Zm6-*adhB* with the plasmid construct pGEMndh::cm^r, carrying a chloramphenicol resistance marker inserted in the AgeI site of *ndh*. Transformation by electroporation and selection of homologous recombinants with the cm^r insert in their chromosomal copy of *ndh* was accomplished following the same procedures as described in [21].

Table 1. Plasmids and strains used in this study.

Strain/Plasmid	Characteristics	Source
pGEMndh::cmr ^r	Plasmid pGEM-Zf(+) derivative, carrying a 2.6 kb DNA fragment between the HindIII and BamHI sites of its MCS, containing a PCR-amplified ORF of the Type II NADH dehydrogenase gene <i>ndh</i> (ZMO_RS04970) with a Cmr marker inserted in its AgeI site	[21]
pNdh	Plasmid pBBR1MCS-2 derivative, carrying a 1.5 kb a 2.6 kb DNA fragment between the HindIII and BamHI sites of its MCS, containing a PCR-amplified ORF of the Type II NADH dehydrogenase gene <i>ndh</i> (ZMO_RS04970) with a Cmr marker inserted in its AgeI site	[6]
Zm6	Wild type, parent strain	ATCC 29191
Zm6- <i>adhB</i>	Zm6 with a Kanr insert in the ORF of the iron-containing alcohol dehydrogenase gene <i>adhB</i> (ZMO_RS07165)	[33]
Zm6- <i>ndh</i>	Zm6 with a Cmr insert in the ORF of respiratory Type II NADH dehydrogenase gene <i>ndh</i> (ZMO_RS04970)	[21]
Zm6- <i>adhB-ndh</i>	Zm6- <i>adhB</i> with a Cmr insert in the ORF of <i>ndh</i>	Present work
Zm6- <i>ndh_pNdh</i>	Zm6- <i>ndh</i> transformed with the pNdh plasmid	[6]
Zm6- <i>cat</i>	Zm6 with a Cmr insert in the ORF of catalase gene <i>cat</i> (ZMO_RS04105)	[34]
Zm6- <i>adhB-cat</i>	Zm6- <i>adhB</i> with a Cmr insert in the ORF of <i>cat</i>	[14]
Zm6- <i>cat_pNdh</i>	Zm6- <i>cat</i> , transformed with the pNdh plasmid	[14]

Strains were maintained and cultivated at 30 °C, without aeration, on medium containing (per 1 L of distilled water) 50 g glucose, 5 g yeast extract, 1.0 g of KH₂PO₄, 1.0 g of (NH₄)₂SO₄, and 0.5 g of MgSO₄ × 7H₂O. Overnight cultivations were produced with added antibiotics (chloramphenicol, 120 µg mL⁻¹ and/or kanamycin, 310 µg mL⁻¹, where required). Cells from overnight cultures were then inoculated at OD₅₅₀ around 0.5 in a fresh medium without antibiotics and used for growth experiments with externally added H₂O₂ after their OD₅₅₀ had reached 2. For platings the same medium composition was used, supplemented with 2 g L⁻¹ of agar.

2.2. Viability Tests for Hydrogen Peroxide Resistance

For viability tests cells were inoculated in fresh medium at OD₅₅₀ of 0.5 and cultivated at 30 °C, without aeration. During exponential growth phase, when the culture OD₅₅₀ had reached around 2, cultures were transferred to 2 mL centrifuge tubes, H₂O₂ was added at 0, 2, or 4 mM final concentration, and incubated at 30 °C for an additional 30 min. To assess the viability after the hydrogen peroxide treatment, for each experimental condition four replicates of serial dilutions of the H₂O₂-treated culture, with OD₅₅₀ ranging from 0.5 to 0.5 × 10⁻⁵ were produced and plated (spotted) on agar plates in 5 µL aliquots.

2.3. Preparation of Cell-Free Extracts, Cytoplasmic Membranes, and Permeabilized Cells

For catalase assays, cell-free extracts were prepared from exponentially growing cultures that had reached OD₅₅₀ around 2. Sedimentation, washing, concentration, and ultrasonic breakage of cells, with following preparation of cell-free extracts, was performed as described previously [34]. For alcohol dehydrogenase assays, cells were permeabilized following the slightly modified procedure of Osman et al. [35], by vortexing a concentrated cell suspension in phosphate buffer in the presence of lysozyme and small amount of

chloroform [36]. For assaying NADH:coenzyme Q₁ oxidoreductase, cytoplasmic membrane vesicles were prepared from cells grown overnight. After sedimentation, washing and resuspension in phosphate buffer, ultrasonic breakage, and removal of unbroken cells, membranes were sedimented by ultracentrifugation. Sedimentation was conducted in a Thermo Scientific Sorvall WX+ Ultracentrifuge at 35,000 r.p.m. for 1.5 h, then the pellet was washed with phosphate buffer, resuspended, and centrifuged repeatedly for 1 h. Finally, the pellet was resuspended in the same buffer to yield a concentrated membrane vesicle suspension with protein concentration in the range of 10–15 mg mL⁻¹.

2.4. Enzymatic Assays

Catalase activity in the cell-free extracts was measured by monitoring absorbance decline at 240 nm [37]. Assay mixture contained 2.9 mL of 100 mM potassium phosphate buffer, pH 7, 100 µL of 1 M hydrogen peroxide, and 20 µL of cell-free extract. The rate of hydrogen peroxide decomposition was calculated using millimolar extinction coefficient 0.0436 mM⁻¹cm⁻¹. The total ADH activity in permeabilized cells was assayed spectrophotometrically, by measuring the increase of NADH absorbance at 340 nm in the presence of ethanol [33], taking 6.22 mM⁻¹cm⁻¹ as the millimolar extinction coefficient. The reaction was started by addition of 10 µL of permeabilized cell suspension to 1.5 mL of 30 mM TrisHCl buffer (pH 8.5), containing 1 M ethanol and 1 mM NAD⁺. AdhA contribution was calculated from assays with 200 mM butanol instead of ethanol, and the result was subtracted from the total ADH activity to find the fraction of AdhB [38]. NADH dehydrogenase (NADH:CoQ₁ oxidoreductase) activity of the respiratory chain was assayed in membrane preparation after the terminal oxidase was inhibited with KCN. Ubiquinone Q₁ was used as the electron acceptor. A total of 1 mL of assay in a spectrophotometer cuvette contained 0.1 M potassium phosphate buffer (pH 7), 5 µL of membranes (10–12 mg mL⁻¹ protein concentration), 10 µL of 8 mM CoQ₁, and 20 µL of 1 M potassium cyanide. Reaction was started by adding 10 µL of 10 mM NADH, and the absorption decrease at 276 nm wavelength was followed spectrophotometrically. For calculations, 14.3 mM⁻¹cm⁻¹ was taken for the millimolar extinction coefficient of oxidized CoQ₁.

2.5. RT-qPCR

Reactants, equipment, and assay for RT-qPCR were essentially the same as previously described by Strazdina et al. [20]. The TRIzolTM reagent (Invitrogen, Thermo Fisher Scientific, Waltham, MA, USA) was used for mRNA purification. Reverse transcription was performed with the Thermo Scientific kit. Maxima SYBR green/ROX qPCR Master Mix (Fermentas, Vilnius, Lithuania) was used for the PCR. The quantitative real-time PCRs (RT-qPCR) were carried out in duplicate in a real-time thermal cycler (Model 7300, Applied Biosystems, Waltham, MA, USA). Amplification conditions were: 50 °C for 2 min and 94 °C for 3 min, followed by 40 cycles with 94 °C for 30 s, 57 °C for 30 s, 72 °C for 30 s. In order to compare *cat* transcription between the strains, RT-qPCR data in all cases were normalized against the respective amounts of cDNA of the housekeeping gene, glyceraldehyde-3-phosphate dehydrogenase (ZMO 0177), applying the 2^{(-Delta Delta C(T))} method for relative quantification [39]. Primers used for quantification of *cat* transcripts were: *kat_f* (AGGGAATTGGGATTTAGTCG), and *kat_r* (AAGAGGAATACCACGATCAG). For glyceraldehyde-3-phosphate dehydrogenase the primers were: *Gapdeh_f* (AAGCTTGCGTTGATATCGT) and *Gapdeh_r* (GTGCAAGATGCGTTAGAAAC) [34].

2.6. Analytical Procedures

Protein concentration in membrane samples was determined according to Markwell et al. [40]. Cell concentration was determined as optical density at 550 nm (OD₅₅₀), and dry cell mass of the suspensions was calculated by reference to a calibration curve. All results represent the mean values of at least 3 experiments (if not stated otherwise), with standard deviations shown as error bars.

3. Results

In the hydrogen peroxide sensitivity assay (Figures 1 and 2), exponentially growing cells after reaching OD₅₅₀ of 2 were harvested by centrifugation in 15 mL Falcon tubes and resuspended at the same cell density (corresponding to the timepoint zero in Figure 1) in 14 mL of fresh growth medium supplemented with H₂O₂. Figure 1A shows a representative experiment, illustrating typical growth curves with several H₂O₂ concentrations in the millimolar range. The average values of specific growth rates of Zm6 and four mutant strains during a 6 h growth period after H₂O₂ addition are presented in Figure 2, based on data from 3–6 experiments with each hydrogen peroxide concentration.

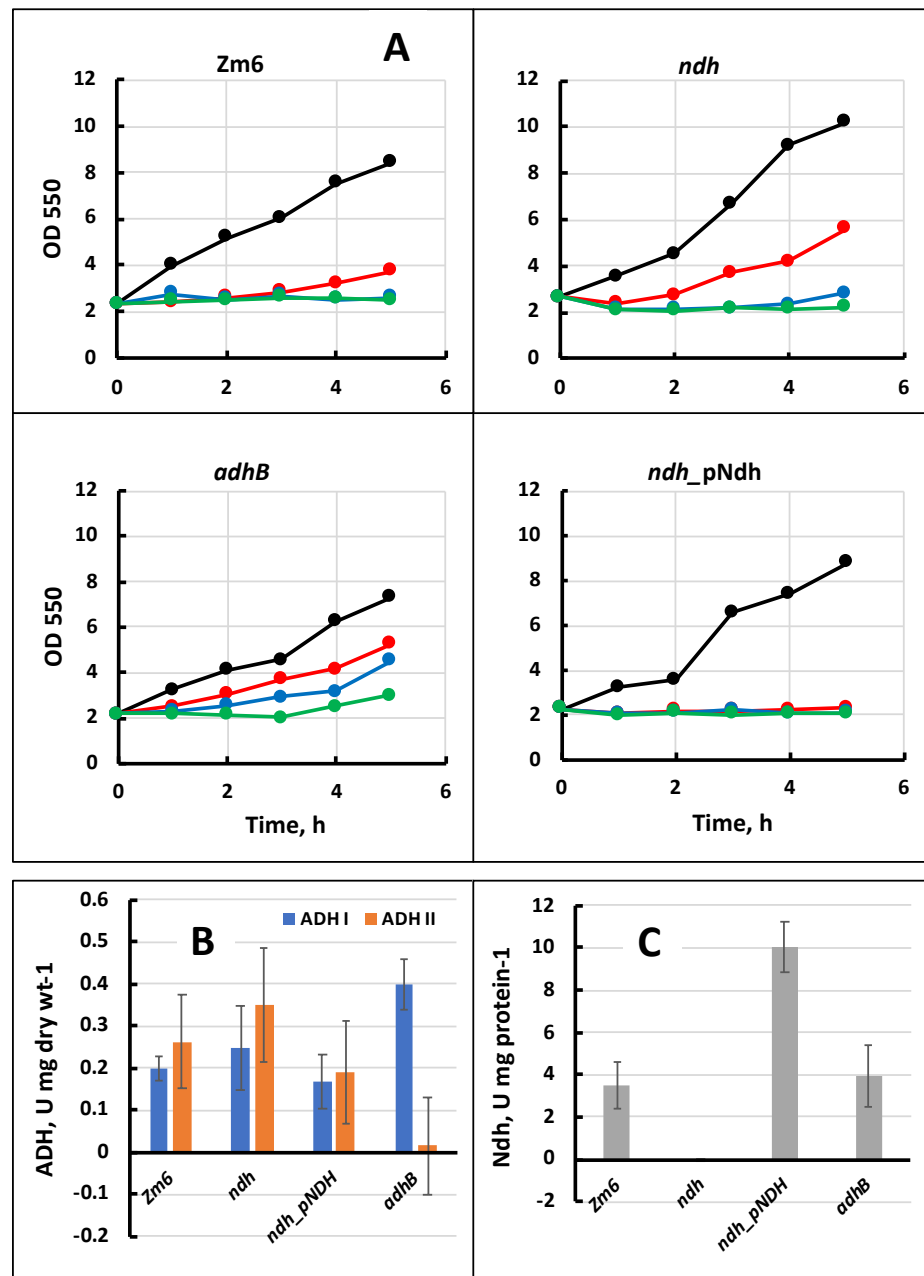


Figure 1. The effect of ADH II and Ndh activities on the growth of *Z. mobilis* strains in the presence of H₂O₂ in the millimolar range. (A), growth of the wild type and mutant strains with H₂O₂ at 0 mM (black), 2 mM (red), 4 mM (blue), and 6 mM (green) final concentration; (B), activity of ADH I and ADH II in permeabilized cells, and (C), activity of NADH:CoenzymeQ₁ oxidoreductase in cell membrane preparations. For details see the text.

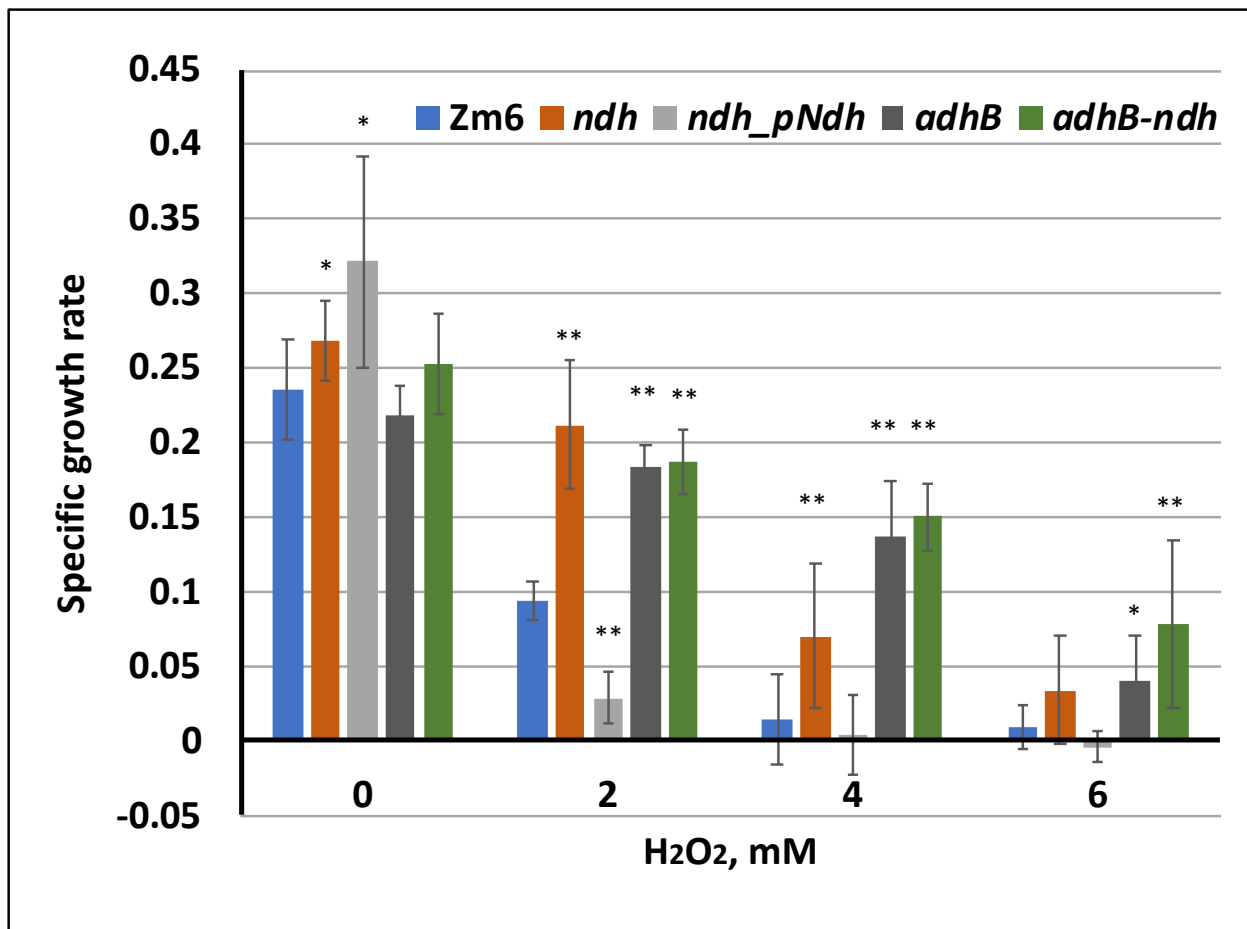


Figure 2. The average specific growth rate (h^{-1}) of the wild type and mutant strains during a period of 6 h after transferring of exponentially growing cells to fresh growth medium, supplemented with hydrogen peroxide. At each H_2O_2 concentration statistical significance of the differences between the Zm6 and mutant growth is shown: * $p < 0.05$; ** $p < 0.01$.

The phenotypes of the *adhB* and *ndh* knock-out mutants, and the *ndh* overexpression from the plasmid construct pNdh, are illustrated in Figure 1B,C; the activities of their membrane NADH:CoQ₁ oxidoreductase and both alcohol dehydrogenase isoenzymes are shown. In the strains Zm6, Zm6-*ndh*, and Zm6-*ndh_pNdh*, the activities of both ADH isoenzymes were in the range of 0.15–0.35 U mg dry wt⁻¹. For Zm6-*adhB*, the activity of ADH II was close to zero, yet the activity of ADH I reached 0.4 U mg dry wt⁻¹. The NADH:CoQ₁ oxidoreductase activity in Zm6-*adhB* was comparable to that in Zm6; in Zm6-*ndh* it was zero, while in Zm6-*ndh_pNdh* it exceeded the wild type level by a factor of 3. Notably, mutant strains strongly differed from the parent strain Zm6 with respect to their hydrogen peroxide sensitivity. In the presence of several millimolar H_2O_2 , the Ndh-negative strain, AdhB-negative strain, and moreover, the double mutant Zm6-*adhB-ndh*, grew significantly better than Zm6. However, complementation of Zm6-*ndh* with the plasmid pNdh (Figure 1C) dramatically decreased the ability to grow in the presence of H_2O_2 . As seen in Figure 2, already with 2 mM H_2O_2 in the culture medium the specific growth rate of Zm6-*ndh_pNdh* was significantly lower than the growth rate of Zm6-*ndh*, and also below that of the parent strain.

Viability tests after treatment of cells with 2 mM or 4 mM H_2O_2 supported the peroxide resistance pattern, shown in Figure 2. Serial dilutions on agar plates are presented in Figure 3. With 2 mM H_2O_2 , the strains Zm6-*ndh*, Zm6-*adhB*, and Zm6-*adhB-ndh* showed higher viability than the parent strain (about two to three orders of magnitude above that

of Zm6), while the viability of Zm6-*ndh*_pNdh had decreased by a similar degree. At 4 mM H₂O₂ these differences were even more pronounced.

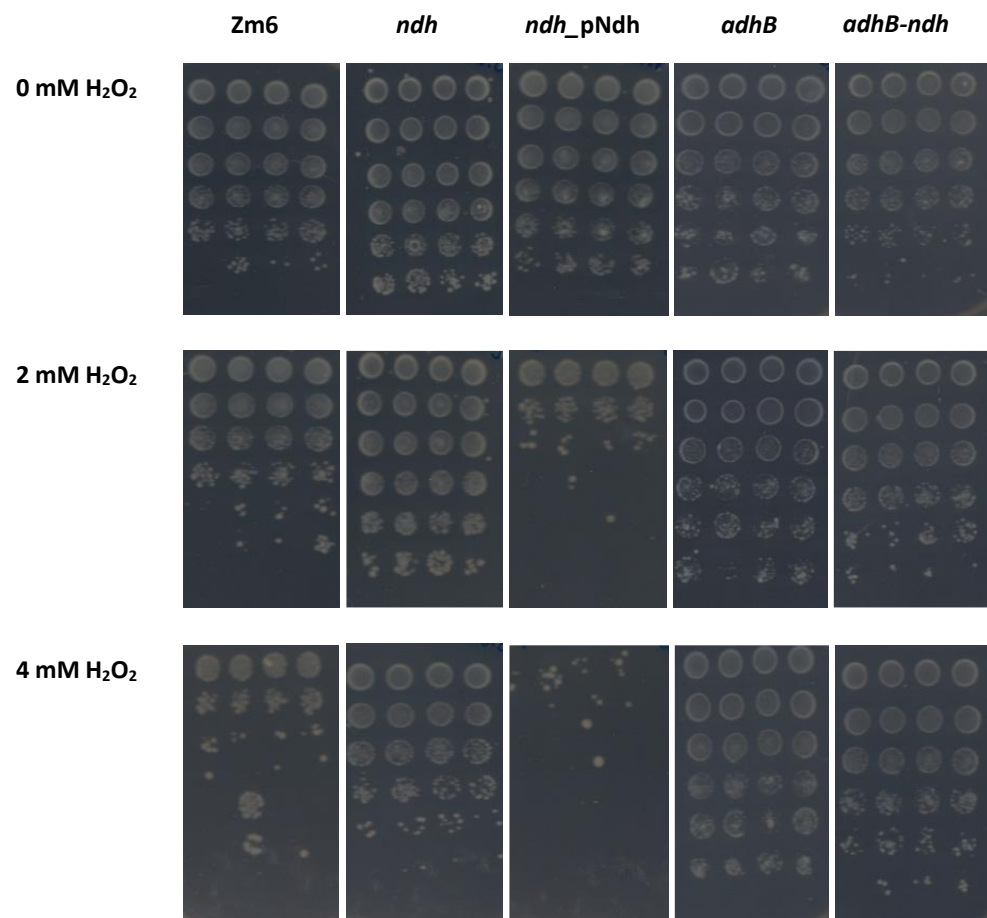


Figure 3. Viability of cells from exponential phase cultures after 30 min incubation with hydrogen peroxide. Serial dilutions ranging from OD 0.5 to 0.5×10^{-5} (from the top to bottom of each panel) were plated on agar plates in four replicates for each strain at each peroxide concentration.

The protection of bacteria against exogenously added H₂O₂ in the millimolar concentration range involves several cellular oxidative defense systems [41], yet catalase is known as the key enzymatic activity for removing H₂O₂ at these concentrations. We examined the catalase activity and the expression level of *cat* gene in the mutant strains (Figure 4). The catalase activity in cell-free extracts of exponentially growing cultures showed a positive correlation with their H₂O₂ resistance. For Zm6-*ndh*, the catalase activity was almost twice the level of the parent strain, while for Zm6-*adhB* and Zm6-*adhB-ndh* it was four and five times above the Zm6 level, respectively. On the other hand, catalase activity in Zm6-*ndh*_pNdh was the lowest: it was below the activity in Zm6. RT-qPCR data showed that the *cat* transcript levels in Zm6-*ndh*, Zm6-*adhB*, and Zm6-*adhB-ndh* were also several times higher than in Zm6 (see the numbers above the bars in Figure 4). The elevated catalase activity in these strains therefore might be largely due to the transcriptional activation of the *cat* gene.

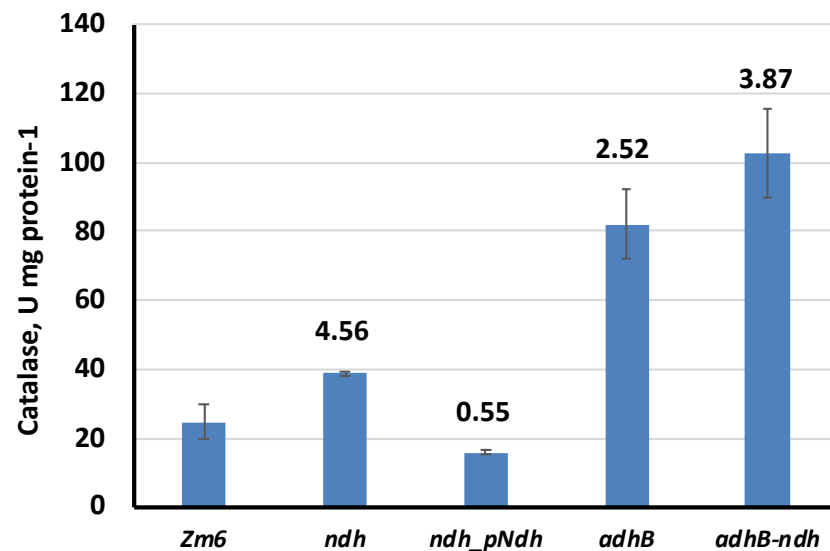


Figure 4. Catalase activity and *cat* gene expression in the mutant strains. Mean data from three experiments are presented. For all mutant strains, catalase activity significantly differs ($p < 0.01$) from that of Zm6. The numbers above the bars show the log₂ fold change of *cat* transcription in the mutants (log₂ (mutant/Zm6)), and represent the mean values of two RT-qPCR experiments, each with two technical repeats.

It thus seemed straightforward to assume that the reason for the different H₂O₂ resistance of the strains could lie in the variation of their catalase activity. To test this hypothesis, we compared H₂O₂ resistance in strains with a *cat*-negative background. The average specific growth rate of Zm6-*cat* at several H₂O₂ concentrations was compared to that of the AdhB-negative strain Zm6-*adhB-cat*, and to the Ndh-overexpressing strain Zm6-*cat_pNdh* (Figure 5).

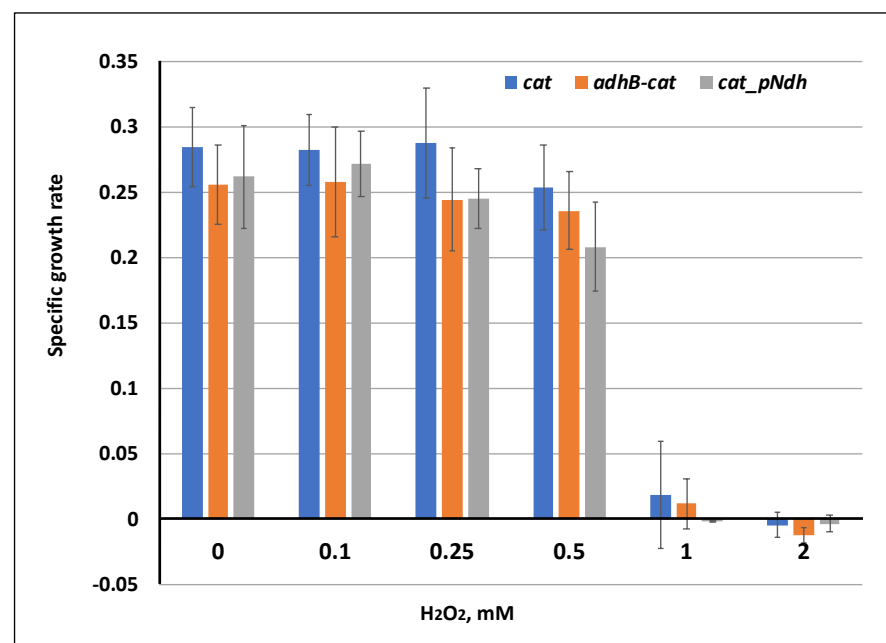


Figure 5. Average specific growth rate (h⁻¹) of the mutant strains with catalase-negative background during a period of 6 h after transferring of cells to fresh growth medium, supplemented with hydrogen peroxide. The differences between the specific growth rates of the strains are not statistically significant at any one of the applied H₂O₂ concentrations.

The strains with *cat* background were more sensitive to exogenous hydrogen peroxide, than the wild type Zm6; they ceased to grow already at 1 mM H₂O₂. However, there were no statistically significant differences in peroxide resistance between them. With a catalase-deficient background, the strain carrying the *adhB* mutation did not show improved growth in the presence of H₂O₂, rather a slight opposite tendency was seen. The peroxide resistance of the Ndh-overexpressing *cat* strain also did not differ significantly from the two other strains. Thus, we concluded that it was the catalase activity that determined the variation of the mutant H₂O₂ resistance within the millimolar (2–6 mM) concentration range.

4. Discussion

In the present study we have demonstrated that the inactivation of two central catabolic enzymes of *Zymomonas mobilis*—the iron-containing alcohol dehydrogenase isoenzyme ADH II (encoded by *adhB*), and/or the respiratory type II NADH dehydrogenase (*ndh*)—substantially elevates the cellular resistance to exogenous hydrogen peroxide in the millimolar concentration range. In the double knock-out mutant Zm6-*adhB-ndh*, the H₂O₂ resistance is even higher than in each of the single mutant strains. These findings reveal some *Z. mobilis* regulatory patterns that differ from other bacteria. What we observe in the *Z. mobilis adhB* strain is quite the opposite to the effects caused by the inactivation of the iron-dependent ADH in *E. coli* and in a number of other bacteria [27–31], where ADH mutation causes a substantial decrease of resistance to exogenously-added H₂O₂.

Z. mobilis is known to possess a respiratory cytochrome peroxidase PerC, supplied with electrons coming from NADH via the Ndh. The knock-out mutant Zm6-*perC* is more sensitive to H₂O₂ than the wild type [25]. Yet, the elevated peroxide resistance of Zm6-*ndh* and the hypersensitivity to H₂O₂ of the Zm6-*ndh_pNdh* strain do not support a NADH-fueled respiratory peroxidase being the key protector of *Z. mobilis* against exogenous H₂O₂. Apparently, other stress-protection systems (primarily catalase) play a more important role, and the putative decrease of the PerC function in the Zm6-*ndh* background is not essential.

The key finding of the present work is the demonstration that the improved H₂O₂-resistance of the mutant strains results from their elevated catalase activity. As expected, strains with *cat* background are more sensitive to exogenous hydrogen peroxide, than the wild type Zm6. The fact that *cat* strains are unable to grow at hydrogen peroxide concentrations above 1 mM demonstrates that catalase in *Z. mobilis* is the dominant hydrogen peroxide protective system for culture growth at 2–6 mM H₂O₂, and that there are no alternative protective systems available for compensating its absence. Importantly, against the catalase-deficient background, the remaining peroxide resistance appears not to depend on the inactivation of AdhB, or overexpression of Ndh. Unlike the iron-containing ADHs in other bacteria, the AdhB in *Z. mobilis* thus seems either not to contribute per se to the oxidative stress protection of the cells, or alternatively, the lack of its protective function in the mutant can be fully compensated (notably, that is not the case, for instance, for *E. coli adhE* mutants at 0.5–1 mM H₂O₂; see [27]).

These observations lead us to a more general question of what the physiological rationale of the dependence of catalase activity on the variation of AdhB and/or Ndh expression might be. We speculate that the rise of catalase might be mitigating the heightened risks of exogenous hydrogen peroxide damage because of the increased availability of NADH in these mutant strains. It is known that free Fe²⁺ reacts with H₂O₂, producing the highly reactive hydroxyl radicals (Fenton reaction) [42]. In *Z. mobilis*, Ndh and AdhB are the dominant catabolic NADH consumers under aerobic and anaerobic condition, respectively. Accordingly, their inactivation should turn more NADH available for non-specific recycling of Fe³⁺ to Fe²⁺, and by that, in the presence of H₂O₂ the Fenton reaction would be maintained and stimulated. Therefore, the enhanced catalase activity in these mutants might well be regarded as a protective reaction against a potential risk of exogenous oxidative stress.

The mutant strains differ as to their transcript levels of the *cat* gene. Although the correlation between the enzymatic activity and the RT-qPCR data on transcription is not perfect (Figure 4), a clear general trend is seen: the levels of *cat* transcript are significantly

higher for *ndh* and *adhB* backgrounds relative to the parent strain Zm6. For the *Z. mobilis adhB* background, a similar increase of *cat* transcript has been recently observed in another work, using a different set of qPCR primers [14]. The mechanisms regulating the differences in the transcription and activity of *cat* in these *Z. mobilis* mutant strains are not clear and would need further study in light of the present findings.

Author Contributions: Conceptualization, U.K.; methodology, K.K., I.S. and N.G.; validation, R.R. and I.S.; formal analysis, U.K. and K.K.; investigation, K.K., I.S., M.B., N.G. and J.M.; resources, U.K. and R.R.; data curation, U.K., M.B. and R.R.; writing—original draft preparation, U.K.; writing—review and editing, U.K., K.K. and M.B.; visualization, U.K. and K.K.; supervision, U.K.; funding acquisition, U.K. All authors have read and agreed to the published version of the manuscript.

Funding: This research was funded by the Latvian Council of Science project lzp-2018/2-0123 and by the Latvian State Education Development Agency ERDF project No.1.1.1.1/18/A/022.

Institutional Review Board Statement: Not applicable.

Informed Consent Statement: Not applicable.

Data Availability Statement: The original contributions presented in the study are included in the article, further inquiries can be directed to the corresponding author.

Conflicts of Interest: The authors declare no conflict of interest.

References

- Rogers, P.L.; Lee, K.J.; Skotnicki, M.L.; Tribe, D.E. Ethanol production by *Zymomonas mobilis*. In *Microbial Reactions; Advances in Biochemical Engineering*; Springer: Berlin/Heidelberg, Germany, 1982; Volume 23, pp. 37–84.
- Sprenger, G. Carbohydrate metabolism in *Zymomonas mobilis*: A catabolic highway with some scenic routes. *FEMS Microbiol. Lett.* **1996**, *145*, 301–307. [[CrossRef](#)]
- Strohdeicher, M.; Neuß, B.; Bringer-Meyer, S.; Sahn, H. Electron transport chain of *Zymomonas mobilis*. Interaction with the membrane-bound glucose dehydrogenase and identification of ubiquinone 10. *Arch. Microbiol.* **1990**, *154*, 536–543.
- Kalnenieks, U.; Galinina, N.; Bringer-Meyer, S.; Poole, R.K. Membrane d-lactate oxidase in *Zymomonas mobilis*: Evidence for a branched respiratory chain. *FEMS Microbiol. Lett.* **1998**, *168*, 91–97. [[CrossRef](#)]
- Rutkis, R.; Galinina, N.; Strazdina, I.; Kalnenieks, U. The inefficient aerobic energetics of *Zymomonas mobilis*: Identifying the bottleneck. *J. Basic Microbiol.* **2014**, *54*, 1090–1097. [[CrossRef](#)] [[PubMed](#)]
- Rutkis, R.; Strazdina, I.; Balodite, E.; Lasa, Z.; Galinina, N.; Kalnenieks, U. The low energy-coupling respiration in *Zymomonas mobilis* accelerates flux in the Entner–Doudoroff pathway. *PLoS ONE* **2016**, *11*, e0153866. [[CrossRef](#)]
- Pentjuss, A.; Odzina, I.; Kostromins, A.; Fell, D.A.; Stalidzans, E.; Kalnenieks, U. Biotechnological potential of respiring *Zymomonas mobilis*: A stoichiometric analysis of its central metabolism. *J. Biotechnol.* **2013**, *165*, 1–10. [[CrossRef](#)]
- Swings, J.; De Ley, J. The biology of *Zymomonas*. *Bacteriol. Rev.* **1977**, *41*, 367–377. [[CrossRef](#)]
- Cazetta, M.L.; Celligoi, M.A.P.C.; Buzato, J.B.; Scarmino, I.S. Fermentation of molasses by *Zymomonas mobilis*: Effects of temperature and sugar concentration on ethanol production. *Biores. Technol.* **2007**, *98*, 2824–2828. [[CrossRef](#)]
- Zhang, M.; Eddy, C.; Deanda, K.; Finkelstein, M.; Picataggio, S. Metabolic engineering of a pentose metabolism pathway in ethanologenic *Zymomonas mobilis*. *Science* **1995**, *267*, 240–243. [[CrossRef](#)]
- Mohagheghi, A.; Linger, J.G.; Yang, S.H.; Smith, H.; Dowe, N.; Zhang, M.; Pienkos, P.T. Improving a recombinant *Zymomonas mobilis* strain 8b through continuous adaptation on dilute acid pretreated corn stover hydrolysate. *Biotechnol. Biofuels* **2015**, *8*, 55. [[CrossRef](#)]
- Yang, S.; Mohagheghi, A.; Franden, M.A.; Chou, Y.C.; Chen, X.; Dowe, N.; Himmel, M.E.; Zhang, M. Metabolic engineering of *Zymomonas mobilis* for 2,3-butanediol production from lignocellulosic biomass sugars. *Biotechnol. Biofuels* **2016**, *9*, 189. [[CrossRef](#)] [[PubMed](#)]
- Qiu, M.; Shen, W.; Yan, X.; He, Q.; Cai, D.; Chen, S.; Wei, H.; Knoshaug, E.P.; Zhang, M.; Himmel, M.E.; et al. Metabolic engineering of *Zymomonas mobilis* for anaerobic isobutanol production. *Biotechnol. Biofuels* **2020**, *13*, 15. [[CrossRef](#)] [[PubMed](#)]
- Kalnenieks, U.; Balodite, E.; Ströhler, S.; Strazdina, I.; Rex, J.; Pentjuss, A.; Fuchino, K.; Bruheim, P.; Rutkis, R.; Pappas, K.M.; et al. Improvement of acetaldehyde production in *Zymomonas mobilis* by engineering of its aerobic metabolism. *Front. Microbiol.* **2019**, *10*, 2533. [[CrossRef](#)] [[PubMed](#)]
- Rogers, P.L.; Jeon, Y.J.; Lee, K.J.; Lawford, H.G. *Zymomonas mobilis* for fuel ethanol and higher value products. *Adv. Biochem. Eng./Biotechnol.* **2007**, *108*, 263–288.
- Wang, X.; He, Q.; Yang, Y.; Wang, J.; Haning, K.; Hu, Y.; Wu, B.; He, M.; Zhang, Y.; Bao, J.; et al. Advances and prospects in metabolic engineering of *Zymomonas mobilis*. *Metab. Eng.* **2018**, *50*, 57–73. [[CrossRef](#)]
- Kalnenieks, U.; Pappas, K.M.; Bettenbrock, K. *Zymomonas mobilis* metabolism: Novel tools and targets for its rational engineering. *Adv. Micr. Physiol.* **2020**, *77*, 37–88.

18. Hayashi, T.; Furuta, Y.; Furukawa, K. Respiration-deficient mutants of *Zymomonas mobilis* show improved growth and ethanol fermentation under aerobic and high temperature conditions. *J. Biosci. Bioeng.* **2011**, *111*, 414–419. [[CrossRef](#)]
19. Hayashi, T.; Kato, T.; Watakabe, S.; Song, W.; Aikawa, S.; Furukawa, K. The respiratory chain provides salt stress tolerance by maintaining a low NADH/NAD⁺ ratio in *Zymomonas mobilis*. *Microbiology* **2015**, *161*, 2384–2394. [[CrossRef](#)]
20. Strazdina, I.; Balodite, E.; Lasa, Z.; Rutkis, R.; Galinina, N.; Kalnenieks, U. Aerobic catabolism and respiratory lactate bypass in Ndh-negative *Zymomonas mobilis*. *Metabol. Eng. Commun.* **2018**, *7*, e00081. [[CrossRef](#)]
21. Kalnenieks, U.; Galinina, N.; Strazdina, I.; Kravale, Z.; Pickford, J.L.; Rutkis, R.; Poole, R.K. NADH dehydrogenase deficiency results in low respiration rate and improved aerobic growth of *Zymomonas mobilis*. *Microbiology* **2008**, *154*, 989–994. [[CrossRef](#)]
22. Melo, A.M.; Bandejas, T.M.; Teixeira, M. New Insights into Type II NAD(P)H:Quinone Oxidoreductases. *Microbiol. Mol. Biol. Rev.* **2004**, *68*, 603–616. [[CrossRef](#)] [[PubMed](#)]
23. Kalnenieks, U.; Balodite, E.; Rutkis, R. Metabolic engineering of bacterial respiration: High vs. low P/O and the case of *Zymomonas mobilis*. *Front. Bioeng. Biotechnol.* **2019**, *7*, 327. [[CrossRef](#)] [[PubMed](#)]
24. Charoensuk, K.; Irie, A.; Lertwattanasakul, N.; Sootsuwan, K.; Thanonkeo, P.; Yamada, M. Physiological importance of cytochrome *c* peroxidase in ethanologenic thermotolerant *Zymomonas mobilis*. *J. Mol. Microbiol. Biotechnol.* **2011**, *20*, 70–82. [[CrossRef](#)] [[PubMed](#)]
25. Balodite, E.; Strazdina, I.; Galinina, N.; McLean, S.; Rutkis, R.; Poole, R.K.; Kalnenieks, U. Structure of the *Zymomonas mobilis* respiratory chain: Oxygen affinity of electron transport and the role of cytochrome *c* peroxidase. *Microbiology* **2014**, *160*, 2045–2052. [[CrossRef](#)]
26. An, H.; Scopes, R.K.; Rodriguez, M.; Keshav, K.F.; Ingram, L.O. Gel electrophoretic analysis of *Zymomonas mobilis* glycolytic and fermentative enzymes: Identification of alcohol dehydrogenase II as a stress protein. *J. Bacteriol.* **1991**, *173*, 5975–5982. [[CrossRef](#)]
27. Echave, P.; Tamarit, J.; Cabisco, E.; Ros, J. Novel antioxidant role of alcohol dehydrogenase E from *Escherichia coli*. *J. Biol. Chem.* **2003**, *278*, 30193–30198. [[CrossRef](#)]
28. Beckham, K.S.H.; Connolly, J.P.R.; Ritchie, J.M.; Wang, D.; Gawthorne, J.A.; Tahoun, A.; Gally, D.L.; Burgess, K.; Burchmore, R.J.; Smith, B.O.; et al. The metabolic enzyme AdhE controls the virulence of *Escherichia coli* O157:H7. *Mol. Microbiol.* **2014**, *93*, 199–211. [[CrossRef](#)]
29. Lin, G.H.; Hsieh, M.C.; Shu, H.Y. Role of Iron-Containing Alcohol Dehydrogenases in *Acinetobacter baumannii* ATCC 19606 Stress Resistance and Virulence. *Int. J. Mol. Sci.* **2021**, *22*, 9921. [[CrossRef](#)]
30. Luong, T.T.; Kim, E.H.; Bak, J.P.; Nguyen, C.T.; Choi, S.; Briles, D.E.; Pyo, S.; Rhee, D.K. Ethanol-induced alcohol dehydrogenase E (AdhE) potentiates pneumolysin in *Streptococcus pneumoniae*. *Infect. Immun.* **2015**, *83*, 108–119. [[CrossRef](#)]
31. Kavanaugh, D.W.; Porrini, C.; Dervyn, R.; Ramarao, N. The pathogenic biomarker alcohol dehydrogenase protein is involved in *Bacillus cereus* virulence and survival against host innate defence. *PLoS ONE* **2022**, *17*, e0259386. [[CrossRef](#)]
32. Tamarit, J.; Cabisco, E.; Aguilar, J.; Ros, J. Differential inactivation of alcohol dehydrogenase isoenzymes in *Zymomonas mobilis* by oxygen. *J. Bacteriol.* **1997**, *179*, 1102–1104. [[CrossRef](#)] [[PubMed](#)]
33. Kalnenieks, U.; Galinina, N.; Toma, M.M.; Pickford, J.L.; Rutkis, R.; Poole, R.K. Respiratory behaviour of a *Zymomonas mobilis* adhB::kanr mutant supports the hypothesis of two alcohol dehydrogenase isoenzymes catalysing opposite reactions. *FEBS Lett.* **2006**, *580*, 5084–5088. [[CrossRef](#)] [[PubMed](#)]
34. Strazdina, I.; Kravale, Z.; Galinina, N.; Rutkis, R.; Poole, R.K.; Kalnenieks, U. Electron transport and oxidative stress in *Zymomonas mobilis* respiratory mutants. *Arch. Microbiol.* **2012**, *194*, 461–471. [[CrossRef](#)]
35. Osman, Y.A.; Conway, T.; Bonetti, S.J.; Ingram, L.O. Glycolytic flux in *Zymomonas mobilis*: Enzyme and metabolite levels during batch fermentation. *J. Bacteriol.* **1987**, *169*, 3726–3736. [[CrossRef](#)]
36. Kalnenieks, U.; Galinina, N.; Toma, M.M. Physiological regulation of the properties of alcohol dehydrogenase II (ADH II) of *Zymomonas mobilis*: NADH renders ADH II resistant to cyanide and aeration. *Arch. Microbiol.* **2005**, *183*, 450–455. [[CrossRef](#)] [[PubMed](#)]
37. Gonzalez-Flecha, B.; Demple, B. Intracellular generation of superoxide as a by-product of *Vibrio harveyi* luciferase expressed in *Escherichia coli*. *J. Bacteriol.* **1994**, *176*, 2293–2299. [[CrossRef](#)]
38. Kinoshita, S.; Kakizono, T.; Kadota, K.; Das, K.; Taguchi, H. Purification of two alcohol dehydrogenases from *Zymomonas mobilis* and their properties. *Appl. Microbiol. Biotechnol.* **1985**, *22*, 249–254. [[CrossRef](#)]
39. Livak, K.J.; Schmittgen, T.D. Analysis of relative gene expression data using real-time quantitative PCR and the 2^{−ΔΔCT} method. *Methods* **2001**, *25*, 402–408. [[CrossRef](#)]
40. Markwell, M.A.; Haas, S.M.; Bieber, L.L.; Tolbert, N.E. A modification of the Lowry procedure to simplify protein determination in membrane and lipoprotein samples. *Anal. Biochem.* **1978**, *87*, 206–210. [[CrossRef](#)]
41. Sen, A.; Imlay, J.A. How Microbes Defend Themselves From Incoming Hydrogen Peroxide. *Front. Immunol.* **2021**, *12*, 667343. [[CrossRef](#)]
42. Brumaghim, J.L.; Li, Y.; Henle, E.; Linn, S. Effects of hydrogen peroxide upon nicotinamide nucleotide metabolism in *Escherichia coli*: Changes in enzyme levels and nicotinamide nucleotide pools and studies of the oxidation of NAD(P)H by Fe(III). *J. Biol. Chem.* **2003**, *278*, 42495–42504. [[CrossRef](#)] [[PubMed](#)]